Revue des Energies Renouvelables Vol. 20 N°2 (2017) 179 - 193
DOI: https://doi.org/10.54966/jreen.v20i2.619

Evaluation of electrical power losses of photovoltaic modules subjected to partial shading conditions in the three climatic regions of Cameroon

Abdouramani Dadjé [1,2*], Noël Djongyang [1] and René Tchinda [3]

[1] Department of Renewable Energy, National Advanced Polytechnic School
University of Maroua, P.O. Box 46 Maroua, Cameroon

[2] School of Geology and Mining Engineering, University of Ngaoundéré Avril
P.O. Box 454 Ngaoundéré, Cameroon

[3] LISIE, Fotso Victor University Institute of Technology
University of Dschang, PO Box 146 Bandjoun, Cameroon

(reçu le 10 Avril 2017 – accepté le 30 Mai 2017)

Résumé - *Cet article traite du comportement de trois types de panneaux photovoltaïques opérant dans des conditions d'ombrage partiel dans les trois zones climatiques du Cameroun. Le phénomène d'ombrage partiel constitue l'un des facteurs qui perturbent radicalement l'énergie électrique produite par les générateurs photovoltaïques. C'est pour contribuer à résoudre ce problème que nous avons modélisé les panneaux PV fonctionnant dans des conditions d'ombrage partiel sous les paramètres climatiques du Cameroun. La méthode analytique combinée à la méthode itérative est utilisée pour la détermination des paramètres du module PV dans des conditions d'ombrage partiel. Des études ont été menées sur une période d'un an dans trois villes, respectivement: Yagoua pour la région soudano-sahélienne, Tchollire dans la région soudanaise et Tibati dans la région équatoriale. Trois types de panneaux PV ont été utilisés {polycristallin (MSX-60), monocristallin (Shell SP70) et couche mince CIS (Shell ST40)}. Les pertes de puissance électrique de chaque type de panneau ont été évaluées.*

Abstract - *This paper studies the behavior of three types of photovoltaic panels operating under partial shading conditions in the three climatic regions of Cameroon. The phenomenon of partial shading constitutes one of the factors which drastically disrupt the electric power produced by the photovoltaic generators. It is to contribute to solve this problem that we modelled the PV panels operating in partial shading conditions under the climatic parameters of the study area. The analytical method combined with the iterative method are used for the determination of PV module parameters under partial shading conditions. Studies were carried out over a period of one year in three cities, respectively: Yagoua for the sudano-sahelian region, Tchollire in the sudanese region and Tibati in the southern equatorial region. Three types of PV panels were used {polycrystalline (MSX-60), monocrystalline (Shell SP70) and CIS thin film (Shell ST40)}. The electrical power losses of each type of panel were evaluated.*

Key Words: Electrical powerlosses - Partial shading conditions - Analytic and iterative methods - Comparative analysis.

1. INTRODUCTION

Greenhouse gas emissions are the main causes of climate change, and among the measures taken to reduce this emissions and slow down the process of global warming, the use of renewable energy appears as the fitting solution. Cameroon which is an emerging country needs a sufficient electrical power both in quality and quantity to achieve its development objective. The hydroelectric source generates more than 75% of energy for national electricity generation. The interconnected North network of Cameroon which has only one dam and the populations are

* abdouramanid@yahoo.fr

undernourished with electricity [1]. Cameroon is a country rich in renewable energy resources. The irradiation is high throughout the country. Its exploitation sometimes requires numerous studies and technical predispositions for optimal performance.

Photovoltaic solar energy is seen as the saving solution for these populations for several reasons: the abundance of solar radiation in this part of the country allows for optimal production, distribution to households and to remote areas where the population are not connected to the hydraulic power network and their Energy problem could be solved by photovoltaic installations. However, the output density of the PV system is low and strongly depends on the state of sunshine and the surface of the photovoltaic array of temperature [2, 3].

PV cells are very sensitive to partial shading. If a cell or part of a module in a serial chain is shaded, then instead of giving the power output, the absorbent shaded cell(s) [4, 5]. The basic photovoltaic cell is modelled by its electrical circuit equivalent to a diode [5, 6]. These methods for estimating energy efficiency based on experimental results and empirical formulations are presented in [5, 7]. The analytical and iterative methods, namely Newton Raphson, are used to obtain optimal parameter determination of photovoltaic panels [8]. This technique is commonly used to estimate the maximum power of photovoltaic generators operating under non-uniform conditions of rapidly varying irradiation [9-11].

To validate the model, we made simulations with the standard values given by the constructors. This test was carried out on the three types of panels that we chose namely the polycrystalline silicon photovoltaic panel, the monocrystalline type and the CIS thin film. The absolute error of 1.51 % obtained between the constructor value and our result leads us to say that the model is good. We then subject the model to partial shading. Subsequently, we introduce the meteorological data of the cities of the area of our study area. From the electric powers obtained, we calculate and see the variation the losses of electric powers for four degrees of shading: 0%, 25%, 50%, and 100%.

Although we are currently experiencing a major phenomenon of climate change; the results obtained during the year 2016 in the three regions are satisfactory. The analysis of these results makes it possible to make predictions in the management of energy in this part of the country throughout the year.

2. LOCATION AND METEOROLOGICAL DATA OF THE STUDY AREA

Cameroon is situated between latitude of 2°N to 13°N, longitude of 9°E to 17°E and covers a land area of about 475 442 km^2. An equatorial climate with four seasons (two dry and two rainy) is found in the southern part and Atlantic Ocean coasts with approximately 3890 mm of precipitation per year. Abundant rainfall occurs from April to November, and practically throughout the year in the south-west mountains (approximately 10 000 mm per year). The climate tends to be of the sahelian type as one leaves the southern to the northern part of the country with two seasons (one dry and one rainy). The dry season lasts from October to April (700 mm of precipitation per year in the central plateau) and the north-west is semi-arid (380 mm of precipitation per year).

Three main climatic regions are found: the southern equatorial region, which extends from 2°N to nearly as far as latitude 6°N; the sudanese region, wet and tropical, extending from 7°N to a little beyond 10°N; the sudano–sahelian region (10–13)°N, dry and tropical. The mean outdoor temperatures vary between 25 °C in the south, 21.1 °C in the central plateau and 32.2 °C in the north [12] . Three cities has been considered for this study {Yagoua (sudano-sahelian region), Tchollire (sudanese region) and Tibati (Southern equatorial region)}.

2.1 Location of study area

Figure 1 and **Table 1** show respectively the study areas and their geographical coordinates

2.2 Meteorological data of the study site

In this section, we present in **Table 2** the meteorological data of the three study areas taken over a two-year period measured monthly from January to December of the year 2015 and 2016. But the rest of our study, will over the period of 2016.

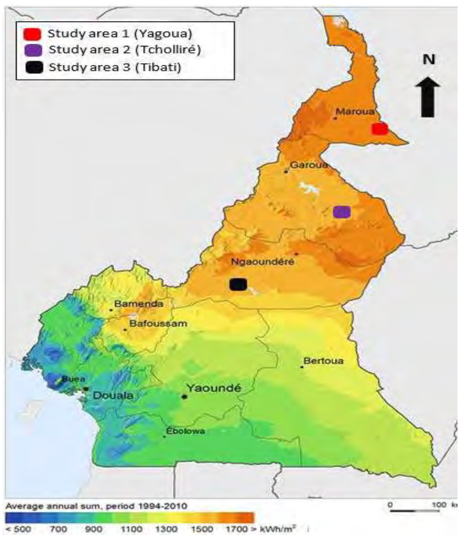

Fig. 1: Locations of study areas: Yagoua, Tchollire, Tibati [13]

Table 1: Geographical coordinates of the study area [14]

City	Yagoua	Tchollire	Tibari
Latitude	10°20'27"N	8°24'0"N	6°28'0"N
Longitude	15°13'58"E	14°10'0"E	12°37'59"N
Elévation	335 m	393 m	859 m

Table 2: Meteorological data (irradiance and temperature) of the three cities sudano-sahelian region (**a**); sudanese region (**b**) and southern equatorial region (**c**)

year	Value	month	jan	feb	mar	apr	may	jun	jul	aug	sept	oct	nov	dec	average
2015	T	AVG (%)	23.3	29.3	32	32.8	33	30.1	27.7	26.5	27.1	28.9	28.4	23.1	28.6
	G	Max (W/m^2)	774	1109.8	1307.5	1305.8	1321.1	1012.4	998.2	906	863.2	906.4	900.1	876.9	1321.1
2016	T	AVG (%)	24.9	29.2	35.7	36	32.5	29.4	28	27.8	28.5	30.7	31.6	28.7	30.2
	G	Max (W/m^2)	752.4	1231.1	1352.2	1330	1325.7	1234.2	997.2	932.4	932.8	1006.4	1003.7	996.5	1352.2

a) Yagoua station (sudano-sahelian region)

year	Value \ month		jan	feb	mar	apr	may	jun	jul	aug	sept	oct	nov	dec	average
2015	T	AVG (%)	25.1	30.9	33	32.9	31.2	27.6	26.6	25.5	25.5	26.8	26	22.9	27.8
	G	Max (W/m2)	840.2	1106.8	1294.3	1101.1	1040.4	1006.2	951.2	900.4	790.1	977.2	982.9	879	1294.3
2016	T	AVG (%)	24.7	28.9	33.4	32	29.9	26.6	26	25.7	26	26.9	27.3	26.8	27.9
	G	Max (W/m2)	780.2	1159	1291.8	1109	1032.2	998.3	950.4	899	792.1	998	997.2	907.5	1291.8

[illegible]

Year	Value \ month		jan	feb	mar	apr	may	jun	jul	aug	sept	oct	nov	dec	average
2015	T	AVG (°C)	22.1	24.8	25.6	24.8	23.6	22.4	22.4	22.4	22	22.4	22.5	21.8	23.1
	G	Max (W/m2)	805.4	815.2	1007.4	980.4	859	708.9	1038.7	1085.7	1100.6	1197.7	958.6	860.8	1197.7
2016	T	AVG (°C)	22.6	24.8	25.5	24.6	23.4	22.5	22.2	22	22.3	22.6	22.9	22.6	23.2
	G	Max (W/m2)	858.4	912	1221	1013.2	1022.6	990.8	1019	1005.9	1007.2	1015	1191.1	1100.7	1221

[illegible]

3. MODELING OF PHOTOVOLTAIC MODULE

The model used is that proposed in the literature by [10, 11] is the model with one diode.

The Kirchhoff 's law allow us to establish the following current-tension equation [4, 10, 11],

$$I = I_{ph} - I_0 . \left(\exp\left(\frac{q(V + R_s I)}{n_1 N_s k T_c} - 1 \right) \right) - \frac{V + R_s I}{R_{sh}} \quad (1)$$

For some reason of simplification R_{sh} is considered too much great. So that, $(V + R_s . I) / R_{sh}$ will not be considered, and then we obtain,

$$I = I_{ph} - I_0 . \left(\exp\left(\frac{q(V + R_s I)}{n N_s k T_c} - 1 \right) \right) \quad (2)$$

The configuration of the PV module is shown in figure 2. The module is a group of 36 cells that is broken down into two subgroups of 18 cells each. The first subgroup is illuminated normally, while the second is shaded with a variable percentage (figure 3).

The bypass diode connected in parallel PV cells subgroups limit the harmful effects of partial shading and improves power output [5, 9, 15].

The total voltage of the circuit V_T is obtained by the {eq. (3)} from V_1, V_2 and V_D as follows:

$$\begin{cases} V_T = V_1 + V_D & \text{if} \quad V_2 < V_D \\ V_T = V_1 + V_2 & \text{if} \quad V_2 > V_D \end{cases} \quad (3)$$

$$V_1 = \left(\frac{n N_s k T_c}{q} \right) \times \ln\left(\frac{I_{ph} - I + I_0}{I_0} \right) \quad (4)$$

$$V_2 = \left(\frac{n N_s k T_c}{q} \right) \times \ln\left(\frac{\beta . I_{ph} - I + I_0}{I_0} \right) \quad (5)$$

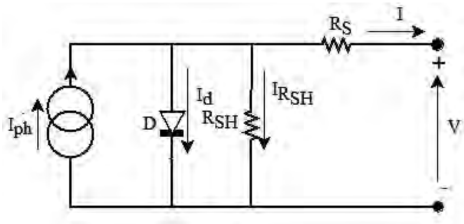

Fig. 2: Circuit equivalent to single-diode for a photovoltaic cell

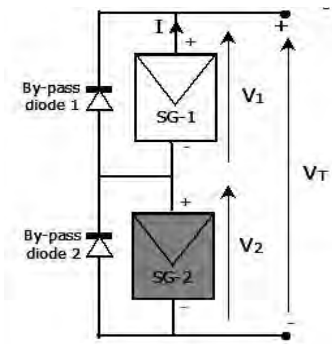

Fig. 3: Configuration of the module into two subgroups of 18 cells each

The photovoltaic current is given by the following relation [4, 16]

$$I_{ph} = \left(I_{sc} + \Delta T \times K_i\right)\left(G / G_r\right) \tag{6}$$

$$I_0 = I_{0ref} \times \left(T_c / T_r\right)^3 \times \exp\left(\frac{q\, E_g \left(\frac{1}{T_r} - \frac{1}{T_c}\right)}{n\, N_s\, k}\right) \tag{7}$$

•**For** $I = 0,\ V = V_{oc}$

$$0 = I_{ph} - I_{0ref} \cdot \left(\exp\left(\frac{q V_{oc}}{n N_s k T_c}\right) - 1\right) \tag{8}$$

$$I_{0ref} = \frac{I_{ph}}{\left(\exp\left(\frac{q V_{oc}}{n N_s k T_c}\right) - 1\right)} \tag{9}$$

After combining equation (8) and (9), we obtain equation (10),

$$I_0 = \frac{I_{ph}}{\exp\left(\frac{q V_{oc}}{n N_s k T_c}\right) - 1} \times \left(T_c / T_r\right)^3 \times \exp\left(\frac{q E_g \left(\frac{1}{T_r} - \frac{1}{T_c}\right)}{n\, N_s\, k}\right) \tag{10}$$

•**For** $I = I_p,\ V = V_{mp}$

$$I_{mp} = I_{ph} - I_0 \left(\exp\left(\frac{q\left(V_{mp} + R_s I_{mp}\right)}{n\, N_s\, k\, T_c} \right) - 1 \right) \tag{11}$$

$$\exp\left(\frac{q\left(V_{mp} + R_s I_{mp}\right)}{n\, N_s\, k\, T_c} \right) = \frac{I_{ph} - I_{mp}}{I_0} + 1 \tag{12}$$

$$R_s = \frac{n\, N_s\, k\, T_c}{q\, I_{mp}} \times \ln\left(\frac{I_{ph} - I_{mp}}{I_0} + 1 \right) - \frac{V_{mp}}{I_{mp}} \tag{13}$$

Derivating each part of the equation (2), we obtain

$$1 = 0 - I_0 \frac{q}{n\, N_s\, k\, T_c} \left(\frac{\partial V}{\partial I} + R_s \right) \exp\left(\frac{q}{n\, N_s\, k\, T_c} (V + R_s\, I) \right) \tag{14}$$

$$1 + I_0 \frac{q\, R_s}{n\, N_s\, k\, T_c} \exp\left(\frac{q(V + R_s\, I)}{n\, N_s\, k\, T_c} \right) = -I_0 \frac{q}{n\, N_s\, k\, T_c} \frac{\partial V}{\partial I} \exp\left(\frac{q(V + R_s\, I)}{n\, N_s\, k\, T_c} \right) \tag{15}$$

$$\frac{\partial V}{\partial I} = -\frac{1 + I_0 \dfrac{q\, R_s}{n\, N_s\, k\, T_c} \exp\left(\dfrac{q(V + R_s\, I)}{n\, N_s\, k\, T_c} \right)}{I_0 \dfrac{q}{n\, N_s\, k\, T_c} \dfrac{\partial V}{\partial I} \exp\left(\dfrac{q(V + R_s\, I)}{n\, N_s\, k\, T_c} \right)} \tag{16}$$

The simplification of equation (16) gives,

$$\frac{\partial V}{\partial I} = -\left(\frac{n\, N_s\, k\, T_c \exp\left(\dfrac{q(V + R_s\, I)}{n\, N_s\, k\, T_c} \right)}{q\, I_0} + R_s \right) \tag{17}$$

$$\frac{\partial V}{\partial I} = -R_s - \frac{n\, N_s\, k\, T_c \exp\left(\dfrac{q(V + R_s\, I)}{n\, N_s\, k\, T_c} \right)}{q\, I_0} \tag{18}$$

$$R_s = -\frac{\partial V}{\partial I} - \frac{n\, N_s\, k\, T_c \exp\left(\dfrac{q(V + R_s\, I)}{n\, N_s\, k\, T_c} \right)}{q\, I_0} \tag{19}$$

•**For** $I = 0;\quad I_0 = I_{0ref};\quad V = V_{oc}$

$$R_s = -\frac{\left(V_{mp} + V_{oc}\right)}{N_s\, I_{mp}} - \frac{n\, N_s\, k\, T_c}{2\, q\, I_{ph}} \tag{20}$$

•**For** $I = I_{mp},\quad V = V_{mp}$

$$\exp\left(\frac{q\left(V_{mp} + R_s I_{mp}\right)}{n\, N_s\, k\, T_c} \right) = \frac{I_{ph} - I_{mp}}{I_0} + 1 \tag{21}$$

$$-\frac{q\,(V_{mp} + R_s\, I_{mp})}{n\, N_s\, k\, T_c} = \ln\left(\frac{I_{ph} - I_{mp}}{I_0} + 1 \right) \tag{22}$$

$$\Leftrightarrow R_s = \frac{n N_s k T_c}{q I_{mp}} \times \ln\left(\frac{I_{ph} - I_{mp}}{I_0} + 1\right) - \frac{V_{mp}}{I_{mp}} \quad (23)$$

After combining equation (23) in (20), we have,

$$\frac{(V_{oc} - V_{mp})}{N_s I_{mp}} - \frac{n N_s k T_c}{q I_{ph}} = \frac{n N_s k T_c}{q I_{mp}} \times \ln\left(\frac{I_{ph} - I_{mp}}{I_0} + 1\right) - \frac{V_{mp}}{I_{mp}} \quad (24)$$

I_0 is of the order 10-3 à 10-7 therefore $\frac{I_{ph} - I_{mp}}{I_0} >> 1$

$$\frac{(V_{oc} - V_{mp})}{N_s I_{mp}} + \frac{V_{mp}}{I_{mp}} = \frac{n N_s k T_c}{q I_{ph}} + \frac{n N_s k T_c}{q I_{mp}} \times \ln(I_{ph} - I_{mp}) - \ln(I_0) \quad (25)$$

$$\left(\frac{V_{oc} - V_{mp}}{N_s} + V_{mp}\right)\frac{(1)}{I_{mp}} = \frac{n N_s k T_c}{q I_{ph}} + \frac{n N_s k T_c}{q I_{mp}} \times \left(\ln(I_{ph} - I_{mp}) - \ln(I_{ph}(T_c / T_r)^3) - \frac{q}{n N_s K}(A - B)\right) \quad (26)$$

Where , $A = E_g\left(\frac{1}{T_r} - \frac{1}{T_c}\right)$ and $B = \frac{V_{oc}}{T_c}$

Put; $X_1 = \left(\frac{V_{oc} - V_{mp}}{N_s} - V_{mp}\right)\frac{1}{I_{mp}}$

$$X_2 = \ln\left((I_{ph} - I_{mp}) - \ln(I_{ph}(T_c / T_r)^3)\right)$$

$$X_3 = E_g\left(\frac{1}{T_r} - \frac{1}{T_c}\right) - \frac{V_{oc}}{T_c}$$

From equation (30), we have

$$X_1 = \frac{n N_s k T_c}{q I_{ph}} + \frac{n N_s k T_c}{q I_{mp}} X_2 - \frac{T_c}{I_{mp}} X_3 \quad (27)$$

$$\Rightarrow X_1 + \frac{T_c}{I_{mp}} X_3 = n\left(\frac{N_s k T_c}{q I_{ph}} + \frac{N_s k T_c}{q I_{mp}} X_2\right) \quad (28)$$

$$n = \frac{X_1 + \frac{T_c}{I_{mp}} X_3}{\frac{N_s k T_c}{q}\left(\frac{1}{I_{ph}} + \frac{X_2}{I_{mp}}\right)} \quad (29)$$

$$n = \frac{q\left(V_{oc} - V_m - \frac{V_{mp}}{N_s} - \frac{V_{oc}}{N_s}\right)}{k T_r \times \left(N_s . I_n\left(\frac{I_{sc} - I_{mp}}{I_{sc}}\right) + \frac{I_{mp}}{I_{sc}}\right)} \quad (30)$$

Then we solve the equation $(V + R_s I) / R_{sh} = 0$ by the iterative method (Newton-Raphson) as shown in figure 4.

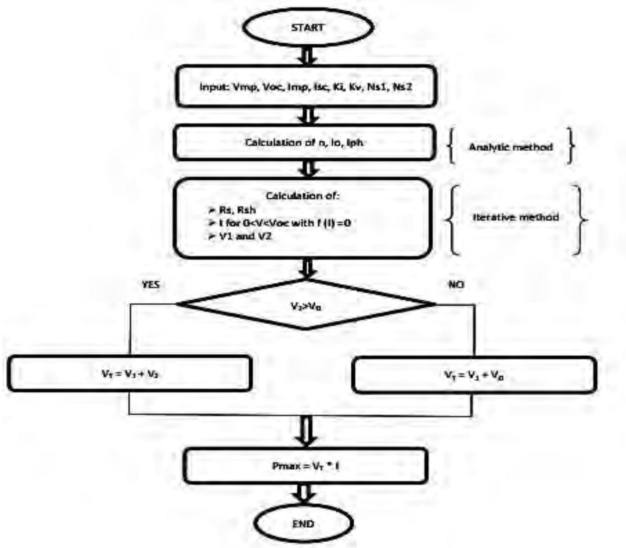

Fig. 4: Flowchart of resolution by the analytical method and the iterative

4. RESULTS AND DISCUSSIONS

Three types of photovoltaic panels are selected with respect to their configuration of 36 cells connected in series: CIS thin film, monocrystalline, polycrystalline. The data used for the simulations are taken from the data sheets of the various manufacturers.

The **Table 3** presents the electrical parameters of the different photovoltaic technologies. [17-19].

Table 3: Electrical characteristics data of the MSX-60, Silicon Shell SP70 and CIS ST40 solar at STC (25 °C, 1.5AM, 1000W/m^2)

Manufacturer data parameters (STC)	Types of modules		
	Polycrystalline MSX-60	Monocrystalline Silicon Shell SP70	CIS thin film Shell ST40
Vmp	17.1	16.5	16.6
Voc	21.1	21.4	23.3
Imp	3.5	4.25	2.41
Isc	3.8	4.7	2.68
Ki	3e-03	2.06e-03	0.35e-03
Kv	-80e-03	-77e -03	-100e -03
Ns	36	36	36

4.1 Test with standard values of manufacturer

We present in figure 5 the results of standard test values of our study.

The result obtained with the standard test values is satisfactory. The maximum power obtained by our model is 59.0921 W as indicated in figure 5(**a**), for the polycrystalline PV panel MSX-60, that is to say a power loss of the order of 1.51 %. Figure 5(**b**) gives curves $I - V$ and $P - V$ of the PV panel under partial shading conditions with shading of 25 %.

This is in accordance with the results obtained by Efstratios *et al.* [6]

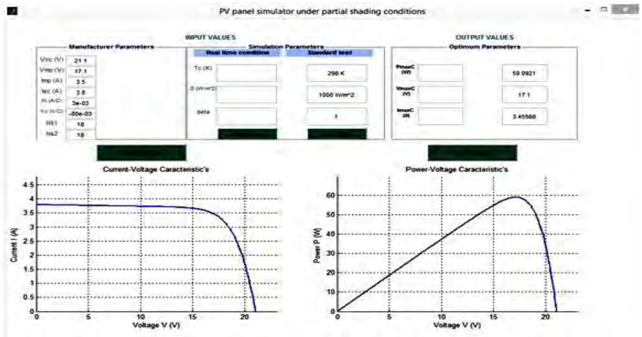

(a)

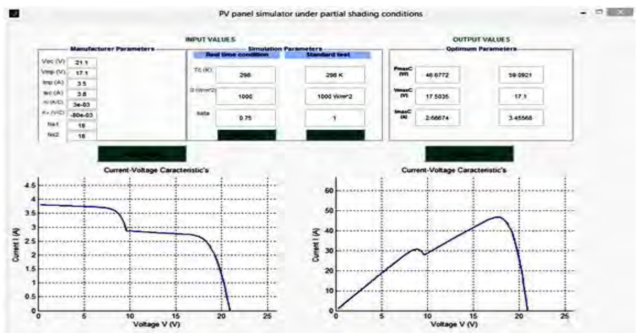

(b)

Fig. 5: Curves for standard test **(a)** and 25% shaded PV panel **(b)**

4.2 Percentage of electrical power losses of the three types of PV panels under shade conditions in the city of Yagoua in 2016

The figure 6 shows the percentage change in the power lost during the year 2016 in the city of Yagoua for the three types of photovoltaic technologies.

In the city of Yagoua, when the photovoltaic panels are fully illuminated, the polycrystalline type presents less power loss compared to the CIS and monocrystalline. At 25% shading, the power losses of the three types of photovoltaic panel are almost identical and are around 20% compared to the standard power expected by the manufacturers. At 50% shade, the losses of the monocrystalline and the CIS are equal to and less than the losses of the polycrystalline panel. At 100% shading, the losses are the same for the three photovoltaic panels and presents the maximum loss.

These power losses are between 48.22% in January and 46.36% in March.

The **Table 4** shows the power loss ratio of the three types of photovoltaic panels.

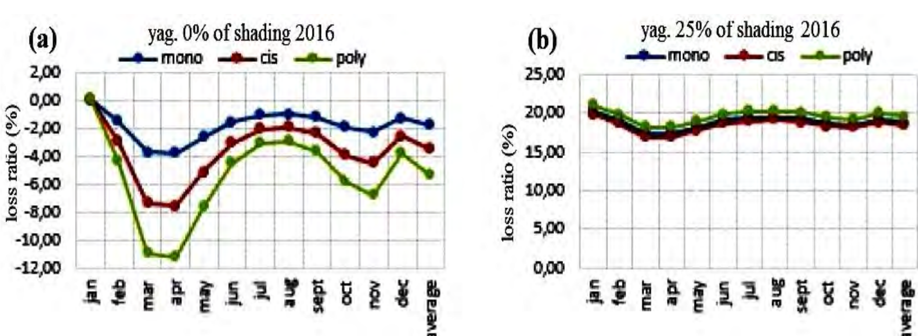

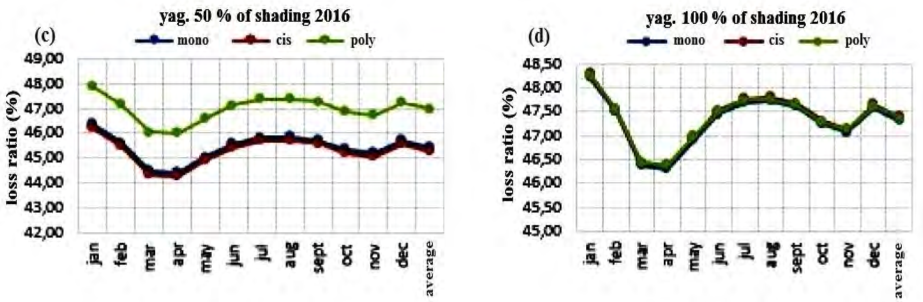

Fig. 6: (**a**), (**b**), (**c**) and (**d**) Yagoua city power losses for the year 2016 at 0%, 25%, 50% and 100% at partial shading

Table 4: Percentage of electrical power losses of the three types of photovoltaic panels (Monocrystalline, CIS Thin Film and Polycrystalline) in Yagoua city for 2016 compared to partial shading rate

Percentage of shading	Constr. Type	jan	feb	mar	apr	may	jun	jul	aug	sept	oct	nov	dec	average
0%	Monocristalin	0.03	-1.45	-3.68	-3.79	-2.58	-1.52	-1.03	-0.96	-1.21	-1.96	-2.27	-1.27	-1.79
	CIS Thin Film	0.03	-1.44	-3.67	-3.77	-2.57	-1.51	-1.03	-0.96	-1.20	-1.96	-2.26	-1.27	-1.78
	Polycristalin	0.03	-1.42	-3.62	-3.72	-2.54	-1.49	-1.01	-0.95	-1.18	-1.93	-2.23	-1.25	-1.76
25%	Monocristalin	20.29	19.13	17.37	17.29	18.23	19.07	19.45	19.51	19.32	18.72	18.48	19.26	18.86
	CIS Thin Film	19.86	18.70	16.96	16.88	17.82	18.65	19.03	19.08	18.89	18.30	18.06	18.84	18.44
	Polycristalin	21.04	19.91	18.21	18.13	19.05	19.86	20.22	20.28	20.09	19.52	19.28	20.04	19.65
50%	Monocristalin	46.37	45.61	44.48	44.42	45.03	45.58	45.82	45.86	45.74	45.35	45.19	45.70	45.44
	CIS Thin Film	46.23	45.47	44.33	44.28	44.90	45.44	45.68	45.72	45.60	45.21	45.05	45.56	45.30
	Polycristalin	47.90	47.16	46.03	45.98	46.59	47.12	47.36	47.40	47.28	46.90	46.74	47.24	46.98
100%	Monocristalin	48.22	47.48	46.36	46.31	46.91	47.45	47.69	47.72	47.60	47.22	47.07	47.57	47.31
	CIS Thin Film	48.29	47.55	46.44	46.38	46.98	47.51	47.75	47.79	47.67	47.29	47.14	47.63	47.38
	Polycristalin	48.26	47.54	46.44	46.39	46.98	47.50	47.74	47.77	47.65	47.28	47.13	47.62	47.37

4.3 Percentage of electrical power loss of the three types of PV panels under shade conditions in the city of Tchollire in 2016

The figure 7 shows the percentage change in the power lost during the year 2016 in the city of Tchollire for the three types of photovoltaic panels.

The climate of Tchollire city shows that at 0% shading the polycrystalline has less loss of power than the CIS and the monocrystalline.

At 25% of the shadow, the results show a slight shift of the polycrystalline on the other two. The polycrystalline type presents more power loss than the other two types of PV panels at a shading percentage equal to 50%.

At 100% shading, the losses are the same for the three photovoltaic panels and presents the maximum loss. These power losses are between 46.76 % in January and 48.63 % in March.

The **Table 5** shows the power loss ratio of the three types of photovoltaic panels.

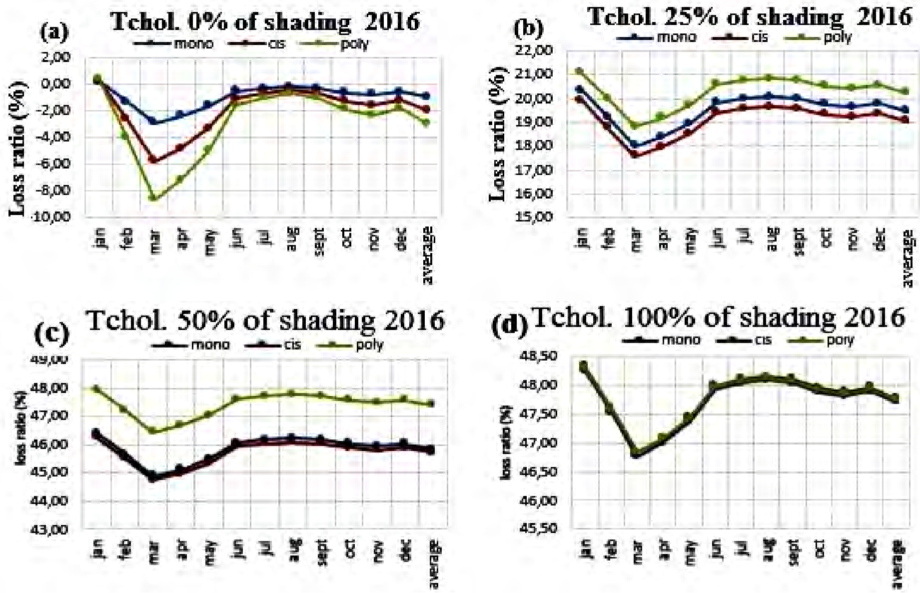

Fig. 7: (**a**), (**b**), (**c**) and (**d**) Tchollire city power losses for the year 2016 at 0%, 25%, 50% and 100% at partial shading

Table 5: Percentage of electrical power losses of the three types of photovoltaic panels (Monocrystalline, CIS Thin Film and Polycrystalline) in Tchollire city for 2016 compared to partial shading rate

Percentage of shading	Constr. Type	jan	feb	mar	apr	may	jun	jul	aug	sept	oct	nov	dec	average
0%	Monocristalin	0.10	-1.34	-2.89	-2.41	-1.69	-0.55	-0.34	-0.24	-0.34	-0.65	-0.79	-0.62	-1.00
	CIS Thin Film	0.10	-1.34	-2.88	-2.40	-1.68	-0.55	-0.34	-0.24	-0.34	-0.65	-0.79	-0.62	-1.00
	Polycristalin	0.10	-1.32	-2.84	-2.37	-1.66	-0.54	-0.34	-0.24	-0.34	-0.64	-0.78	-0.61	-0.98
25%	Monocristalin	20.35	19.21	17.99	18.37	18.94	19.83	19.99	20.07	19.99	19.75	19.64	19.78	19.48
	CIS Thin Film	19.91	18.78	17.58	17.95	18.52	19.40	19.56	19.64	19.56	19.32	19.21	19.35	19.05
	Polycristalin	21.09	19.99	18.81	19.18	19.73	20.59	20.75	20.83	20.75	20.51	20.41	20.54	20.25
50%	Monocristalin	46.40	45.67	44.88	45.12	45.49	46.07	46.17	46.23	46.17	46.02	45.95	46.03	45.84
	CIS Thin Film	46.26	45.53	44.74	44.98	45.35	45.93	46.04	46.09	46.04	45.88	45.81	45.90	45.70
	Polycristalin	47.93	47.21	46.43	46.67	47.04	47.61	47.71	47.76	47.71	47.55	47.48	47.57	47.38
100%	Monocristalin	48.25	47.53	46.75	46.99	47.35	47.92	48.03	48.08	48.03	47.87	47.80	47.89	47.70
	CIS Thin Film	48.31	47.59	46.82	47.06	47.42	47.99	48.09	48.14	48.09	47.94	47.87	47.95	47.77
	Polycristalin	48.29	47.58	46.82	47.06	47.41	47.97	48.07	48.12	48.07	47.92	47.85	47.94	47.75

4.4 Percentage of electrical power loss of the three types of PV panels under shade conditions in the city of Tibati in 2016.

The figure 8 shows the percentage change in the power lost during the year 2016 in the city of Tibati for the three types of photovoltaic technologies.

In the city of Tibati, the monocrystalline type has less power losses than other types at 0% shading.

At 25% it is the CIS which has fewer power losses. At 50% the power losses of the polycrystalline and monocrystalline are identical and lower than those of the CIS.

From 100% shading, the power losses of the three types are identical. We do not recommend the choice of PV panel of polycrystalline types in this area.

The **Table 6** shows the power loss ratio of the three types of photovoltaic panels.

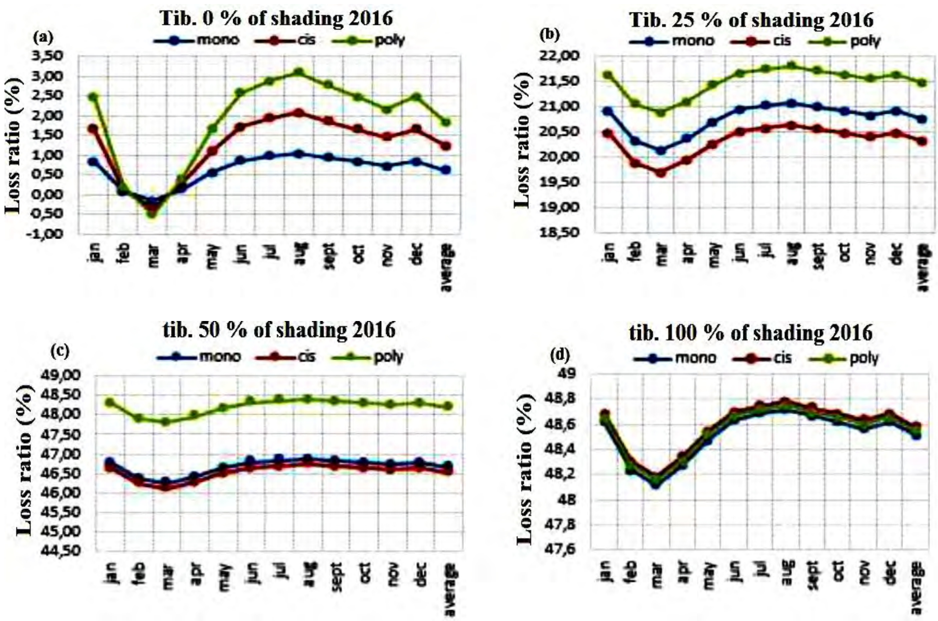

Fig. 8: (**a**), (**b**), (**c**) and (**d**) Tibati city power losses for the year 2016 at 0%, 25%, 50% and 100% at partial shading

Table 6: Percentage of electrical power losses of the three types of photovoltaic panels (Monocrystalline, CIS Thin Film and Polycrystalline) in Tibati city for 2016 compared to partial shading rate

Percentage of shading	Constr. Type	jan	feb	mar	apr	may	jun	jul	aug	sept	oct	nov	dec	average
0%	Monocrystalline	0.83	0.07	-0.17	0.14	0.55	0.86	0.96	1.03	0.93	0.83	0.72	0.83	0.62
	CIS Thin Film	0.82	0.07	-0.17	0.14	0.55	0.86	0.96	1.03	0.93	0.82	0.72	0.82	0.62
	Polycrystalline	0.81	0.07	-0.17	0.14	0.54	0.85	0.95	1.02	0.91	0.81	0.71	0.81	0.61
25%	Monocrystalline	20.91	20.32	20.13	20.37	20.70	20.94	21.02	21.08	21.00	20.91	20.83	20.91	20.75
	CIS Thin Film	20.48	19.89	19.70	19.94	20.26	20.51	20.59	20.64	20.56	20.48	20.40	20.48	20.32
	Polycrystalline	21.64	21.06	20.88	21.11	21.43	21.66	21.74	21.80	21.72	21.64	21.56	21.64	21.48
50%	Monocrystalline	46.77	46.38	46.26	46.42	46.63	46.79	46.84	46.88	46.82	46.77	46.72	46.77	46.67
	CIS Thin Film	46.63	46.25	46.12	46.28	46.49	46.65	46.70	46.74	46.69	46.63	46.58	46.63	46.53
	Polycrystalline	48.30	47.92	47.80	47.95	48.16	48.31	48.37	48.40	48.35	48.30	48.25	48.30	48.19
100%	Monocrystalline	48.61	48.23	48.11	48.27	48.47	48.63	48.68	48.72	48.66	48.61	48.56	48.61	48.51
	CIS Thin Film	48.68	48.30	48.18	48.33	48.54	48.69	48.74	48.78	48.73	48.68	48.62	48.68	48.57
	Polycrystalline	48.65	48.27	48.16	48.31	48.51	48.66	48.71	48.75	48.70	48.65	48.60	48.65	48.55

4.5 Synthesis of the lost power of the three types of photovoltaic panels during the hottest periods of the year in the three cities

The **Table 7** shows the percentage of loss of electric power during the hottest periods of the year.

This synthesis in **Table 7** represents the hottest periods during one year in the three cities of the northern Cameroon. It emerges that the production of photovoltaic electricity in the month of April is favorable.

We find that during the hottest months of the year, the three region show similar results. However, the technology that has the most losses in percentage of electrical power is polycrystalline.

On the other hand, Monocrystalline is the technology of panels with a low percentage of loss of electrical power. This technology of photovoltaic panels is the most advisable for the northern region of Cameroon as well as for the Sahel region in general.

Table 7: Percentage ratio of the loss of electrical power in the three cities during the hottest periods

		Yagoua				Tchollire				Tibati			
Percentage of shading	**Constr. Type**	**mar**	**apr**	**may**	**average**	**mar**	**apr**	**may**	**average**	**mar**	**apr**	**may**	**average**
0%	**Monocrystalline**	-3.68	-3.79	-2.58	-3.35	-2.89	-2.41	-1.69	-2.33	-0.17	0.14	0.55	0.17
	CIS Thin Film	-3.67	-3.77	-2.57	-3.34	-2.88	-2.40	-1.68	-2.32	-0.17	0.14	0.55	0.17
	Polycrystalline	-3.62	-3.72	-2.54	-3.29	-2.84	-2.37	-1.66	-2.29	-0.17	0.14	0.54	0.17
25%	**Monocrystalline**	17.37	17.29	18.23	17.63	17.99	18.37	18.94	18.43	20.13	20.37	20.70	20.40
	CIS Thin Film	16.96	16.88	17.82	17.22	17.58	17.95	18.52	18.02	19.70	19.94	20.26	19.97
	Polycrystalline	18.21	18.13	19.05	18.46	18.81	19.18	19.73	19.24	20.88	21.11	21.43	21.14
50%	**Monocrystalline**	44.48	44.42	45.03	44.64	44.88	45.12	45.49	45.16	46.26	46.42	46.63	46.44
	CIS Thin Film	44.33	44.28	44.90	44.50	44.74	44.98	45.35	45.02	46.12	46.28	46.49	46.30
	Polycrystalline	46.03	45.98	46.59	46.20	46.43	46.67	47.04	46.71	47.80	47.95	48.16	47.97
100%	**Monocrystalline**	46.36	46.31	46.91	46.53	46.75	46.99	47.35	47.03	48.11	48.27	48.47	48.28
	CIS Thin Film	46.44	46.38	46.98	46.60	46.82	47.06	47.42	47.10	48.18	48.33	48.54	48.35
	Polycrystalline	46.44	46.39	46.98	46.60	46.82	47.06	47.41	47.10	48.16	48.31	48.51	48.33

5. CONCLUSION

This study consisted of evaluating the electrical power losses for photovoltaic panels operating under partial shading conditions in the three climatic regions of Cameroon.

To achieve this objective, a new simplified model has been developed to optimize photovoltaic cells. This proposed analytical and numerical model uses the data provided by the manufacturer as the basic data. Three types of solar modules (multi crystalline silicon, mono crystalline silicon and the CIS Thin Film) were modelled and evaluated. The accuracy of the model is also analysed by comparing the manufacturer's data with the results of the simulation.

The results obtained demonstrate the effectiveness of the proposed modelling approach. From the analysis of the curves, it appears that the month of April is very favourable for the production of photovoltaic electrical energy throughout the northern part of Cameroon.

Losses of electrical power are the lowest in the year regardless of the degree of shading. We note that the production of electricity by the photovoltaic panels is very influenced by the climate and the percentage of shade.

But the evolution of the power losses stabilizes at a maximum of 49% regardless of the percentage change in shading. The result of this work allows knowledge of power losses which will result in good management of electrical energy in Cameroon.

Acknowledgments - The authors would like to thank the Regional Meteorological Service Manager of the Adamawa Region and his colleagues from the Northern and Extreme North Regions for providing the data for this study.

NOMENCLATURE

G , Irradiance of the module	G_r , Reference irradiance, $1000 W/m^2$
$V_1 . V_2$, Voltage of unshaded sub-module and voltage of shaded sub-module, A	$I_1 . I_2$, Current of unshaded sub-module and current of shaded sub-module, A
I_D , Diode current, A	I_{mp} , Current at the MPP, A
I_{max} , Maximum cell current, A	I_0 , Reverse saturation current, A
$I_{0.ref}$, Ref.reverse saturation current, A	I_{ph} , Light current, A
$I_{ph.ref}$, Light reference current, A	I_{ref} , Reference current, A0
I_{sc} ,Short circuit current, A	k , Boltzman's constant, 1.381×10^{-23}J/k
MPP, Maximum power point, W	MPPT, Maximum PP tracking, W
n , Ideality factor of the diode	N_s , Number of cells in series
P , PV module power of the module	I , Current of the PV module, A
PV , Photovoltaic	q , Charge of an electron
R_s , Series resistor, Ω	R_{sh} , Shunt resistor, Ω
STC, Standard test conditions	T_c , Current temperature, °C or K
T_r , Reference temperature, 25°C/298K	V , Voltage of the PV module, V
V_D , Voltage of the diode, V	V_{mp} , Voltage at the MPP, V
V_{oc} , Open circuit voltage, V	β , Shading factor, %

REFERENCES

[1] D.K. Kidmo, S.Y. Doka, R. Danwé and N. Djongyang, '*Performance Assessment of Two parameter Weibull Distribution Methods for Wind Energy Applications in the District of Maroua in Cameroon*', International Journal of Sciences: Basic and Applied Research - IJSBAR, Vol. 17, N°1, pp. 39 - 59, 2014.

[2] F. K. Mbakop, N. Djongyang and D. Raïdandi, '*One - dimensional TiO_2/SiO_2 Photonic Crystal Filter For Thermo photovoltaic Applications*' Journal of the European Optical Society-Rapid Publications, Springer, 2016.

[3] F.K. Mbakop, N. Djongyang, G.W. Ejuh, P. Woafo and D. Raïdandi, '*Transmission of Light Through an Optical Filter of a One-Dimensional Photonic Crystal: Application to the Solar Thermophotovoltaic System*', Physica B: Condensed Matter, Vol. 516, pp. 92 - 99, 2017.

[4] C. Deline, D. Aron, J. Steven, M. Jenya and M. Donovan, '*A Simplified Model of Uniform Shading in Large Photovoltaic Arrays Solar Energy*', Solar Energy, Vol. 96, pp. 274 - 282, 2013.

[5] A. Dadjé, N. Djongyang, J.D. Kana, R. Tchinda, '*Maximum Power Point Tracking Methods for Photovoltaic Systems Operating Under Partially Shaded or Rapidly Variable Insolation Conditions: A Review Paper*', International Journal of Sustainable Engineering, Vol. 9, N°4, pp. 224 - 239, 2016.

[6] Efstratios I. Batzelis, Iason A. Routsolias and Stavros A. Papathanassiou, '*An Explicit PV String Model Based on the Lambert Function and Simplified MPP Expressions for Operation Under Partial Shading*', IEEE Transactions on Sustainable Energy, Vol. 5, N°1, pp. 301 - 31, 2014.

[7] L. Sandrolini, M. Artioli and U. Reggiani, '*Numerical Method for the Extraction of Photovoltaic Module Double-Diode Model Parameters through Cluster Analysis*', Applied Energy, Vol. 87, N°2, pp. 442 - 451, 2010.

[8] R. Zieba Falama, A. Dadjé, N. Djongyang and S.Y. Doka, '*A New Analytical Modeling Method for Photovoltaic Solar Cells Based on Derivative Power Function*', Journal of Fundamental and Applied Sciences, Vol. 8, N°2, pp. 426 - 437, 2016.

[9] Giuseppina Ciulla V.L. Brano and V.D. Dio. G. Cipriani, '*A Comparison of Different One-Diode Models for the Representation of I–V Characteristic of a PV Cell*', Renewable and Sustainable Energy Reviews, Vol. 32, pp. 684 - 696, 2014.

[10] K. Vandana, B.K. Das. B. Dinesh, Vandana and P.K. Singh, '*A three Diode Model for Industrial Solar Cells and Estimation of Solar Cell Parameters Using PSO Algorithm*', Renewable Energy, Vol. 78, N°6, pp. 105 - 113, 2015.

[11] B. Alsayid, '*Modeling and Simulation of Photovoltaic Cell/Module/Array with Two-Diode Model*', International Journal of Computer Technology and Electronics Engineering, IJCTEE, Vol. 1, N°3, pp. 6 - 11, 2012.

[12] N. Djongyang and R. Tchinda, '*An Investigation Into Thermal Comfort and Residential Thermal Environments in the Inter tropical Sub-Saharan Africa Region: Field Study Report during the Harmattan Season in Cameroon*', Energy Conversion and Management, Vol. 51, pp. 1391 - 1397, 2010.

[13] http://solargis.com/assets/graphic/free-map/DNI/Solargis-Cameroon-DNI-solar-resourcemap-en.png

[14] https://www.keskeces.com/villes/cameroun/

[15] S. Vemuru, P. Singh and M. Niamat, '*Modelling Impact of Bypass Diodes on Photovoltaic Cell Performance Under Partial Shading*', IEEE, 2012 IEEE International Conference on Electro/Information Technology (EIT), 6-8 May 2012.

[16] J.P. Ram and N. Rajasekar, '*A New Global Maximum Power Point Tracking Technique for Solar Photovoltaic (PV) System Under Partial Shading Conditions (PSC)*', Energy, Vol. 118, N°C, pp. 512 - 525, 2017.

[17] https://www.solarelectricsupply.com/media/custom/upload/Solarex-MSX64.pdf

[18] http://www.solenerg.com.br/files/SP70.pdf

[19]http://www.physics.arizona.edu/~cronin/Solar/TEP%20module%20spec%20sheets/ShellST40.